EMPIRICAL BAYES TRANSDUCTIVE META-LEARNING WITH SYNTHETIC GRADIENTS

Anonymous authors
Paper under double-blind review

ABSTRACT

We propose a meta-learning approach that learns from multiple tasks in a transductive setting, by leveraging unlabeled information in the query set to learn a more powerful meta-model. To develop our framework we revisit the empirical Bayes formulation for multi-task learning. The evidence lower bound of the marginal log-likelihood of empirical Bayes decomposes as a sum of local KL divergences between the variational posterior and the true posterior of each task. We derive a novel amortized variational inference that couples all the variational posteriors into a meta-model, which consists of a synthetic gradient network and an initialization network. The combination of local KL divergences and synthetic gradient network allows for backpropagating information from unlabeled data, thereby enabling transduction. Our results on the Mini-ImageNet and CIFAR-FS benchmarks for episodic few-shot classification outperform previous state-of-the-art methods.

1 INTRODUCTION

While supervised learning of deep neural networks can achieve or even surpass human-level performance (He et al., 2015; Devlin et al., 2018), they can hardly extrapolate the learned knowledge beyond the domain where the supervision is provided. The problem of solving rapidly a new task after learning several other similar tasks is called *meta-learning* (Schmidhuber, 1987; Bengio et al., 1991; Thrun & Pratt, 1998); typically, the data is presented in a two-level hierarchy such that each data point at the higher level is itself a dataset associated with a task, and the goal is to learn a *meta-model* that generalizes across tasks. In this paper, we focus on *few-shot learning* (Vinyals et al., 2016), an instance of meta-learning problems, where a task t, in *meta-testing*, consists of an *unlabeled set* $x_t := \{x_{t,i}\}_{i=1}^n$ and a *labeled set* (aka *support set*) $d_t^l := \{(x_{t,i}^l, y_{t,i}^l)\}_{i=1}^{n^l}$, and the goal is to predict the corresponding labels, namely $y_t = \{y_{t,i}\}_{i=1}^n$, for the unlabeled set. In *meta-training*, y_t is provided as ground truth. The set $d_t := (x_t, y_t)$ is sometimes referred to as *query set*.

A particular important distinction to make is whether each task is solved in a *transductive* or *inductive* manner. The inductive setting is what was originally proposed by Vinyals et al. (2016): we use d_t^l to train a model and test it on x_t (one example at a time). Transduction, however, has the advantage of being able to see all points in x_t before making predictions. We argue that the transductive setting is more relevant to the problem since, as in semi-supervised learning, an inductive learner can always be built from a transductive one (Chapelle et al., 2006). In fact, Nichol et al. (2018) notice that most of the existing meta-learning methods follow the transductive setting unintentionally since they use x_t implicitly via the *batch normalization* (Ioffe & Szegedy, 2015).

Due to the hierarchical structure of the data, it is natural to formulate meta-learning as an instance of *hierarchical Bayes* (HB) (Good, 1980; Berger, 1985), or alternatively, empirical Bayes (EB) (Robbins, 1985; Kucukelbir & Blei, 2014). The difference is that the latter restricts the learning of meta-parameters to point estimates. In this paper, we focus on the EB model, since it largely simplifies the training and testing without losing the strength of the HB formulation.

The idea of using HB or EB for meta-learning is not new: Amit & Meir (2018) derive an objective similar to that of HB using PAC-Bayesian analysis; Grant et al. (2018) show that MAML (Finn et al., 2017) can be understood as a EB method; Ravi & Beatson (2018) consider a HB extension to MAML and compute posteriors via amortized variational inference. However, unlike our proposal, these methods do not take advantage of the unlabeled set. Roughly speaking, they construct the variational

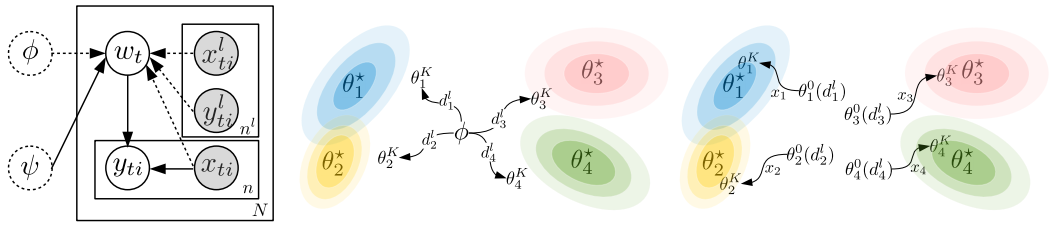

(a) Graphical model of EB (b) MAML (c) Our method (SIB)

Figure 1: **(a)** The generative and inference processes of the empirical Bayes model are depicted in solid and dashed arrows respectively, where the meta-parameters are denoted by dashed circles due to the point estimates. A comparison between MAML (6) and our method (SIB) (9) is shown in **(b)** and **(c)**. MAML is an inductive method since, for a task t, it first constructs a variational posterior $q_{\theta_t^K}$ as a function of the labeled set d_t^l, and then test on the unlabeled set x_t; while SIB constructs a better variational posterior as a function of both d_t^l and x_t: it starts from an initialization $\theta_t^0(d_t^l)$, and then yields θ_t^K by running K synthetic gradient steps on x_t.

posterior as a function of the labeled set d_t^l without taking advantage of the unlabeled set x_t. The situation is similar in gradient based meta-learning methods (Finn et al., 2017; Ravi & Larochelle, 2016; Li et al., 2017b; Nichol et al., 2018; Flennerhag et al., 2019) and many other meta-learning methods (Vinyals et al., 2016; Snell et al., 2017; Gidaris & Komodakis, 2018), where the mechanisms used to generate the task-specific parameters rely on groundtruth labels, thus, there is no place for the unlabeled set to contribute. We argue that this is a suboptimal choice, which may lead to overfitting when the labeled set is small and hinder the possibility of zero-shot learning (when the labeled set is not provided). An exception is Liu et al. (2018). They reuse the label propagation algorithm (Zhu et al., 2003) for transductive inference within each task and show that transduction is useful for boosting the performance.

In this paper, we propose to use synthetic gradient (Jaderberg et al., 2017) to enable transductivity, such that the variational posterior is implemented as a function of the labeled set d_t^l and the unlabeled set x_t. The synthetic gradient is produced by a neural network and learned to be a surrogate of the true gradient. The optimization process is similar to the inner gradient descent in MAML, but it iterates on the unlabeled set x_t rather than on labeled set d_t^l, since it does not rely on y_t to compute the true gradient. The labeled set for an unseen task is now optional, which is only used to generate the initialization in our case. In summary, our main contributions are the following:

1. In section 2 and section 3, we develop a novel empirical Bayes formulation with transduction for meta-learning. To perform amortized variational inference, we propose a parameterization for the variational posterior based on synthetic gradient descent, which incoporates the contextual information from all the inputs of the query set.
2. In section 4, we show in theory that a transductive variational posterior yields better generalization performance. Besides, we show that the proposed empirical Bayes formulation is equivalent to the information bottleneck principle considered by Achille & Soatto (2017). We thus call our method *synthetic information bottleneck* (SIB).
3. In section 5, we verify our proposal empirically. Our experimental results demonstrate that our method significantly outperforms the state-of-the-art meta-learning methods on standard few-shot classification benchmarks.

2 META-LEARNING WITH TRANSDUCTIVE INFERENCE

The goal of meta-learning is to train a *meta-model* on a collection of tasks, such that it works well on another disjoint collection of tasks. Suppose that we are given a collection of N tasks for training. The associated data is denoted by $\mathcal{D} := \{d_t := (x_t, y_t)\}_{t=1}^N$. In the case of few-shot learning, we are given in addition a support set d_t^l for each task. In this section, we revisit the classical empirical Bayes model for meta-learning. Then, we propose to use a transductive scheme in the variational inference by constructing the variational posterior as a function of x_t.

2.1 EMPIRICAL BAYES MODEL

Due to the hierarchical structure among data, it is natural to consider a hierarchical Bayes model with the marginal likelihood

$$p(\mathcal{D}) = \int_{\psi} p(\mathcal{D}|\psi)p(\psi) = \int_{\psi} \Big[\prod_{t=1}^{N} \int_{w_t} p(d_t|w_t)p(w_t|\psi)\Big]p(\psi). \tag{1}$$

The generative process is illustrated in Figure 1 (left, in solid arrows): first, a *meta-parameter* ψ (aka hyper-parameter) is sampled from the *hyper-prior* $p(\psi)$; then, for each task, a *task-specific parameter* w_t is sampled from the *prior* $p(w_t|\psi)$; finally, the dataset is drawn from the *likelihood* $p(d_t|w_t)$. Without loss of generality, we assume the log-likelihood model factorizes as

$$\begin{aligned} \log p_f(d_t|w_t) &= \sum_{i=1}^{n} \log p_f(y_{t,i}|x_{t,i}, w_t) + \log p(x_{t,i}|w_t), \\ &= -\frac{1}{n}\sum_{i=1}^{n} \ell_t\big(\hat{y}_{t,i}(f(x_{t,i}), w_t), y_{t,i}\big) + \text{ constant}, \end{aligned} \tag{2}$$

which is the setting advocated by Minka (2005), in which the generative model $p(x_{t,i}|w_t)$ can be safely ignored since it is irrelevant to the prediction of y_t. To simplify the presentation, we still keep the notation $p(d_t|w_t)$ for the likelihood of the task t and use ℓ_t to specify the discriminative model, which is also referred to as the *task-specific loss*, e.g., the cross entropy loss. The first argument in ℓ_t is the prediction, denoted by $\hat{y}_{t,i} = \hat{y}_{t,i}(f(x_{t,i}), w_t)$, which depends on the *feature representation* $f(x_{t,i})$ and the *task-specific weight* w_t.

Note that rather than following a fully Bayesian approach, we leave some random variables to be estimated by a frequentist approach, e.g., f is a *meta-parameter* of the likelihood model shared by all tasks, for which we use a point estimate. As such, the posterior inference about these variables will be largely simplified. For the same reason, we derive the *empirical Bayes* (Robbins, 1985; Kucukelbir & Blei, 2014), which interprets ψ in a frequentist way:

$$p_{\psi,f}(\mathcal{D}) = \prod_{t=1}^{N} \int_{w_t} p_f(d_t|w_t)p_{\psi}(w_t). \tag{3}$$

We highlight the meta-parameters as subscripts of the corresponding distributions to distinguish from random variables. Indeed, we are not the first to formulate meta-learning as empirical Bayes. The overall model formulation is essentially the same as the ones considered by Amit & Meir (2018); Grant et al. (2018); Ravi & Beatson (2018).

2.2 AMORTIZED INFERENCE WITH TRANSDUCTION

As in standard probabilistic modeling, we derive an *evidence lower bound* (ELBO) on the log version of (3) by introducing a variational distribution $q_{\theta_t}(w_t)$ for each task with parameter θ_t:

$$\log p_{\psi,f}(\mathcal{D}) \geq \sum_{t=1}^{N} \Big[\mathbb{E}_{w_t\sim q_{\theta_t}}\big[\log p_f(d_t|w_t)\big] - D_{\mathrm{KL}}\big(q_{\theta_t}(w_t)\|p_{\psi}(w_t)\big)\Big]. \tag{4}$$

The variational inference amounts to maximizing the ELBO with respect to $\theta_1, \ldots, \theta_N$, which together with the maximum likelihood estimation of the meta-parameters, we have the following optimization problem:

$$\min_{\psi,f} \min_{\theta_1,\ldots,\theta_N} \frac{1}{N}\sum_{t=1}^{N} \Big[\mathbb{E}_{w_t\sim q_{\theta_t}}\big[-\log p_f(d_t|w_t)\big] + D_{\mathrm{KL}}\big(q_{\theta_t}(w_t)\|p_{\psi}(w_t)\big)\Big]. \tag{5}$$

However, the optimization in (5), as N increases, becomes more and more expensive in terms of the memory footprint and the computational cost. We therefore wish to bypass this heavy optimization and to take advantage of the fact that individual KL terms indeed share the same structure. To this end, instead of introducing N different variational distributions, we consider a parameterized family of distributions in the form of $q_{\phi(\cdot)}$, which is defined implicitly by a deep neural network ϕ taking

as input either d_t^l or d_t or both, that is, $q_{\phi(d_t^l)}$ or $q_{\phi(d_t^l,d_t)}$. This technique is known as *amortized* variational inference in the literature (Kingma & Welling, 2013; Rezende et al., 2014).

Since d_t^l and x_t are disjoint, the inference scheme is *inductive* with a variational posterior $q_{\phi(d_t^l)}$. As an example, MAML (Finn et al., 2017) is an inductive method forcing $q_{\phi(d_t^l)}$ to be a Dirac delta distribution, where $\phi(d_t^l) = \theta_t^K$, the K-th iterate of the stochastic gradient descent

$$\theta_t^{k+1} = \theta_t^k + \eta \nabla_\theta \mathbb{E}_{w_t \sim q_{\theta_t^k}} \Big[\log p(d_t^l | w_t) \Big] \text{ with } \theta_t^0 = \phi. \tag{6}$$

Note that we overload ϕ to be both the learnable initialization as well as the amortization.

In this work, we consider a *transductive* inference scheme by using the entire x_t to define the variational posterior as $q_{\phi(x_t)}$. Replacing each q_{θ_t} by $q_{\phi(x_t)}$, (5) can be written as

$$\min_{\psi,f} \min_{\phi} \frac{1}{N} \sum_{t=1}^{N} \Big[\mathbb{E}_{w_t \sim q_{\phi(x_t)}} \big[\log p_f(d_t | w_t) \big] - D_{\mathrm{KL}} \big(q_{\phi(x_t)}(w_t) \| p_\psi(w_t) \big) \Big]. \tag{7}$$

It is also possible to define the variational posterior as $q_{\phi(x_t,y_t)} \equiv q_{\phi(d_t)}$. However, to be consistent with testing, we do not take y_t as input since for which we do not have access to during testing.

In fact, nothing prevents us to come up with an even better variational posterior $q_{\phi(x_t,d_t^l)}$, shown in dashed arrows in Figure 1 (a), which is again transductive by definition. In a nutshell, the meta-model includes f, ψ from empirical Bayes and the amortization ϕ for inference.

3 VARIATIONAL INFERENCE WITH SYNTHETIC GRADIENTS

It is however non-trivial to design a network architecture to implement the amortization $\phi(x_t)$ directly since x_t is itself a dataset. The strategy adopted by *neural processes* (Garnelo et al., 2018) is to aggregate the information from all individual examples via a permutation invariant function. However, as pointed out by Kim et al. (2019), such a strategy tends to underfit x_t because the aggregation does not necessarily attain the most relevant information for identifying the task-specific parameter. Attentive neural process (Kim et al., 2019) may alleviate this issue with a time complexity of $O(n^2)$ while the original neural processes only need $O(n)$ time. We instead design a neural network $\phi(x_t)$ to parameterize the optimization process of θ_t. More specifically, consider a stochastic gradient descent on θ_t for optimizing (5) with step size η:

$$\theta_t^{k+1} = \theta_t^k - \eta \nabla_{\theta_t} D_{\mathrm{KL}} \Big(q_{\theta_t^k}(w) \,\|\, p_{\psi,f}(w \mid d_t) \Big). \tag{8}$$

We would like to parameterize this optimization dynamics up to the K-th step via $\phi(x_t)$, such that $q_{\theta_t^K}$ is a good approximation of the optimum $q_{\theta_t^\star}$. It consists of parameterizing

$$\text{(a) the } \textbf{initialization} \ \theta_t^0 \text{ and (b) the } \textbf{gradient} \ \nabla_{\theta_t} D_{\mathrm{KL}}(q_{\theta_t}(w_t) \,\|\, p_{\psi,f}(w_t | d_t)).$$

By doing so, θ_t^K becomes a function of ϕ, ψ and x_t[1], we therefore realize $q_{\phi(x_t)}$ as $q_{\theta_t^K}$.

For (a), we opt to either let $\theta_t^0 = \lambda$ to be a global data-independent initialization as in MAML (Finn et al., 2017) or let $\theta_t^0 = \lambda(d_t^l)$ with a few supervisions from the support set, where λ can be implemented by a permutation invariant network described in Gidaris & Komodakis (2018). In the second case, the features of the support set will be first averaged in terms of their labels and then scaled by a learned vector of the same size.

For (b), the fundamental reason that we parameterize the gradient is because we do not have access to y_t during the meta-testing phase. Note that we are able to follow (8) in meta-training to obtain $q_{\theta_t^\star}(w_t) \propto p_f(d_t|w_t) p_\psi(w_t)$. To make a consistent parameterization in both meta-training and meta-testing, we thus discard y_t when constructing the variational posterior. Regarding the true gradient, a key observation is that, under a reparameterization $w_t = w_t(\theta_t, \epsilon)$ with $\epsilon \sim p(\epsilon)$,

$$\nabla_{\theta_t} D_{\mathrm{KL}} \Big(q_{\theta_t} \| p_{\psi,f} \Big) = \mathbb{E}_\epsilon \Big[\frac{1}{n} \sum_{i=1}^{n} \frac{\partial \ell_t(\hat{y}_{t,i}, y_{t,i})}{\partial \hat{y}_{t,i}} \frac{\partial \hat{y}_{t,i}}{\partial w_t} \frac{\partial w_t(\theta_t, \epsilon)}{\partial \theta_t} \Big] + \nabla_{\theta_t} D_{\mathrm{KL}} \Big(q_{\theta_t} \| p_\psi \Big),$$

[1] θ_t^K is also dependent of f. We deliberately remove this dependency to simplify the update of f.

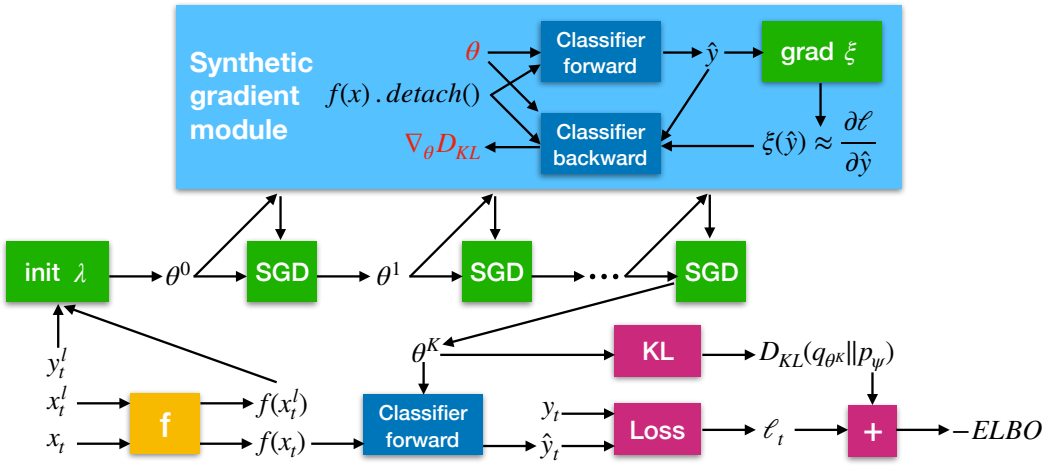

Figure 2: The computation graph to compute the negative ELBO, where the input and output of the synthetic gradient module are highlighted in red. The detach() is used to stop the back-propagation down to the feature network. Note that we do not include every computation for simplicity.

where all the terms can be computed without y_t except for $\frac{\partial \ell_t}{\partial \hat{y}_{t,i}}$, thus, we introduce a deep neural network $\xi(\hat{y}_{t,i})$ to synthesize it. The idea of synthetic gradients was originally proposed by Jaderberg et al. (2017) to parallelize the back-propagation. Here, the purpose of $\xi(\hat{y}_{t,i})$ is to update θ_t regardless of the groundtruth labels, which is slightly different from its original purpose. Besides, we do not introduce an additional loss to force $\xi(\hat{y}_{t,i})$ to approximate $\frac{\partial \ell_t}{\partial \hat{y}_{t,i}}$ since $\xi(\hat{y}_{t,i})$ will be learned to yield a reasonable θ_t^K even without mimicking the true gradient.

To sum up, we have derived a particular implementation of $\phi(x_t)$ by parameterizing the ideal mean-field update, namely (8), with respect to the query set d_t, where the meta-model ϕ includes an initialization network λ and a synthetic gradient network ξ, such that the output of the amortization $\phi(x_t)$ is θ_t^K – the K-th iterate of the following update:

$$\theta_t^{k+1} = \theta_t^k - \eta \left[\mathbb{E}_\epsilon \left[\frac{1}{n} \sum_{i=1}^{n} \xi(\hat{y}_{t,i}) \frac{\partial \hat{y}_{t,i}}{\partial w_t} \frac{\partial w_t(\theta_t^k, \epsilon)}{\partial \theta_t} \right] + \nabla_{\theta_t} D_{\mathrm{KL}} \left(q_{\theta_t^k} \| p_\psi \right) \right]. \tag{9}$$

The overall algorithm is depicted in Algorithm 1. We also make a side-by-side comparison with MAML shown in Figure 1. Rather than viewing (9) as an optimization process, it may be more precise to think of it as a part of the computation graph created in the forward-propagation. The computation graph of the amortized inference is shown in Figure 2,

As an extension, if we were deciding to estimate the feature network f in a Bayesian manner, we would have to compute higher-order gradients as in the case of MAML. This is inpractical from a computational point of view and needs technical simplifications (Nichol et al., 2018). By introducing a series of synthetic gradient networks in a way similar to Jaderberg et al. (2017), the computation will be decoupled into computations within each layer, and thus becomes more feasible. We see this as a potential advantage of our method and leave this to our future work[2].

4 Generalization of Empirical Bayes and its Connection to Information Bottleneck

In this section, we study the generalization ability of the empirical Bayes (EB) model as well as its connection to the information bottleneck principle proposed by Achille & Soatto (2017).

[2]We do not insist on Bayesian estimation of the feature network because most Bayesian versions of CNNs underperform their deterministic counterparts.

Algorithm 1 Variational inference with synthetic gradients for empirical Bayes

Input: the dataset $\mathcal{D}$; the step size η; the number of inner iterations K; pretrained f.
Initialize the meta-models ψ, and $\phi = (\lambda, \xi)$.
while not converged **do**
    Sample a task t and the associated dataset d_t (plus optionally the support set d_t^l).
    Compute the initialization $\theta_t^0 = \lambda$ or $\theta_t^0 = \lambda(d_t^l)$.
    for $k = 1, \ldots, K$ **do**
        Compute θ_t^k via (9).
    end for
    Compute $w_t = w_t(\theta_t^K, \epsilon)$ with $\epsilon \sim p(\epsilon)$.
    Update $\psi \leftarrow \psi - \eta \nabla_\psi D_{\mathrm{KL}}(q_{\theta_t^K(\psi)} \| p_\psi)$.
    Update $\phi \leftarrow \phi - \eta \nabla_\phi D_{\mathrm{KL}}(q_{\phi(x_t)} \| p_f \cdot p_\psi)$.
    Optionally, update $f \leftarrow f + \eta \nabla_f \log p_f(d_t | w_t)$.
end while

From (3), we can see that EB implies a) $\{d_t\}_{t=1}^N$ are independent of each other and b) a decomposition of the joint distribution (see Appendix A for the derivation)

$$p_{\psi,f}(w_1, \ldots, w_N, \mathcal{D}) = \prod_{t=1}^{N} p_{\psi,f}(w_t | d_t) p_{\psi,f}(d_t). \tag{10}$$

Thus, rather than viewing $w_1, \ldots, w_N$ as N different random variables, we may view $\{(w_t, d_t)\}_{t=1}^N$ as iid samples drawn from $p_{\psi,f}(w, d) = p_{\psi,f}(w|d)p_{\psi,f}(d)$[3], which, by variational inference, will be approximated by its variational counterpart $q(w, d) = q(d)q(w|d)$, where $q(d)$ can be seen as the underlying data distribution and $q(w|d)$ is the variational posterior.

Consider an amortization $\phi(d)$ and $d = (x, y)$, then we can parameterize the variational posterior as $q(w|d) = q_{\phi(d)}(w)$, or even simpler: $q(w|d) = q(w|x) = q_{\phi(x)}(w)$. Note that both parameterizations result in transductive inference since, if we would like to test on x, we will incorporate x to build a variational posterior. An inductive variational posterior is a special case such that $q(w|d, d^l) = q(w|d^l) = q_{\phi(d^l)}(w)$.

Before going into details, we first introduce a few notations: the *entropy* is defined as $H_p(\mathrm{x}) := \mathbb{E}_{p(\mathrm{x})}[-\log p(\mathrm{x})]$; the *mutual information* is given by $I_p(\mathrm{x}; \mathrm{y}) := D_{\mathrm{KL}}\big(p(\mathrm{x}, \mathrm{y}) \| p(\mathrm{x})p(\mathrm{y})\big)$; the *cross entropy* is defined as $H_{p,q}(\mathrm{x}) := \mathbb{E}_{p(\mathrm{x})}[-\log q(\mathrm{x})]$.

Assuming that $q(w|d)$ can be optimized exactly to match the empirical Bayes model, we can then use it as a proxy to analyze the generalization performance of EB. Certainly, the quality of the optimization matters, we will also analyze this effect.

To this end, we first identify the empirical risk for a single task as $L(w, d) := \frac{1}{n}\sum_{i=1}^n \ell_t(\hat{y}_i(f(x_i), w), y_i)$. Then, the average empirical risk is the expectation over all possible samples and weights, which depends on the variational posterior and the data distribution:

$$\hat{R}(q(w|d), q(d)) := \mathbb{E}_{d\sim q(d)}\mathbb{E}_{w\sim q(w|d)} L(w, d) \tag{11}$$

The true risk should be independent of any particular variational posterior. Inspired by Xu & Raginsky (2017), we define the true risk as follows, where we sample the task-specific weight from the *aggregated posterior* $q(w)$:

$$\begin{aligned} R(q(w), q(d)) &:= \mathbb{E}_{w\sim q(w)}\mathbb{E}_{t\sim q(t)}\mathbb{E}_{(x_{t,i}, y_{t,i})} \ell_t(\hat{y}_{t,i}(f(x_{t,i}), w), y_{t,i}) \\ &= \mathbb{E}_{w\sim q(w)}\mathbb{E}_{t\sim q(t)}\mathbb{E}_{d\sim q(d|t)} \frac{1}{n}\sum_{t=1}^{n} \ell_t(\hat{y}_i(f(x_i), w), y_i) \\ &= \mathbb{E}_{w\sim q(w)}\mathbb{E}_{d\sim q(d)} L(w, d). \end{aligned} \tag{12}$$

Finally, the generalization error is defined as

$$\mathrm{gen}(q(w|d), q(d)) := R(q(w), q(d)) - \hat{R}(q(w|d), q(d)). \tag{13}$$

[3]When the context is clear, we ignore the parameters and write $p_{\psi,f}(w, d) = p(w, d)$.

Intuitively, the generalization error measures how much the empirical risk concentrated on the true risk is. That is, we would like to bound the tail of the distribution over all possible values of the empirical risk. By taking an expectation of the objective in (7) with respect to the choice of $\mathcal{D}$, we have $\mathbb{E}_{\mathcal{D}}[\frac{1}{N}\sum_{t=1}^{N} D_{\mathrm{KL}}(q(w_t|d_t)\|p(d_t|w_t)p(w_t))] = \mathbb{E}_{d\sim q(d)} D_{\mathrm{KL}}(q(w|d)\|p(d|w)p(w))$. We show in Theorem 1 that the quantity on the right hand side directly affects the generalization performance.

Theorem 1. *Given distributions $q(w|d)$, $q(d)$, $p(w)$ and $p(d|w)$, if $\ell_t(\hat{y}(w), y)$ is σ-subgaussian for all w, the following inequalities hold:*

$$\mathbb{E}_{d\sim q(d)} D_{KL}\Big(q(w|d)\|p(d|w)p(w)\Big) \geq I_q(w;d) + H_{q,p}(d|w) \tag{14}$$
$$\geq \frac{n}{2\sigma^2} gen(q(w|d), q(d))^2 + \hat{R}(q(w|d), q(d));$$
$$\mathbb{E}_{d\sim q(d)} D_{KL}\Big(q(w|d)\|p(w|d)\Big) \leq D_{KL}\Big(q(w,d)\|p(w,d)\Big). \tag{15}$$

The equality in (14) holds if $q(w) = p(w)$. The equality in (15) holds if $q(d) = p(d)$.

The proof of Theorem 1 can be found in Appendix B.

Implications of (14) The inequality (14) basically says that (7) can be seen a regularized empirical risk minimization in which the regularization term is an upper bound of the mutual information between the weight and the sample. In general, there is a tradeoff between the generalization error and the empirical risk controlled by the coefficient $\frac{n}{2\sigma^2}$, where $n = |d|$ is the cardinality of d. If n is small, then we are in the overfitting regime. This is the case of the inductive inference with variational posterior $q(w|d^l)$, where the support set d^l is fairly small by the definition of few-shot learning. Consequently, we expect these methods to have large generalization errors in light of the above analysis. On the other hand, if we were following the transductive setting, the sample size n would be larger and thus would achieve a small generalization error. However, keeping increasing n will potentially over-regularize the model and thus yield negative effect. An empirical study on varying n can be found in Table 4 in the Appendix. Besides, the inequality (14) also suggests that the quality of the variational inference, measured by $\mathbb{E}_{d\sim q(d)} D_{\mathrm{KL}}(q(w|d)\|p(w|d))$, largely affect the generalization error. If we can make this term diminishing to zero, we will achieve zero generalization error.

Besides, (14) reveals a connection between empirical Bayes and information bottleneck (Tishby et al., 2000; Achille & Soatto, 2017). The right hand side of (14) is exactly the IB objective considered by Achille & Soatto (2017) with a coefficient equal to 1. This connection is critical to the analysis since the generalization error is introduced by invoking its relationship to $I(w;d)$. We find this connection interesting, thus, we call our method *synthetic information bottleneck* (SIB).

Implications of (15) An obvious message from the inequality (15) is that, if we choose appropriate likelihood, prior and variational posterior such that $p(w,d)$ is aligned with $q(w,d)$, the empirical Bayes model can actually be pretty good, that is, both the generalization error and the empirical risk are close to zero. If we look at the message more carefully, it also implies that a good likelihood is the key to represent the data well; the inference model is less important as long as the aggregated posterior coincides with the prior. A similar empirical finding was confirmed by Gidaris et al. (2019), who suggests to learn a better feature model, which in turn leads to a good likelihood model according to the definition in (2).

5 EXPERIMENTS

In this section, we first validate our method on few-shot learning, and then on zero-shot learning. Note that many meta-learning methods, such as MAML, cannot do zero-shot learning since they rely on the support set.

5.1 FEW-SHOT CLASSIFICATION

We compare SIB with state-of-the-art methods on few-shot classification problems. Our code is available at `https://bit.ly/2CHHR3F`.

Method	Backbone	MiniImageNet, 5-way 1-shot	MiniImageNet, 5-way 5-shot	CIFAR-FS, 5-way 1-shot	CIFAR-FS, 5-way 5-shot
Matching Net (Vinyals et al., 2016)	Conv-4-64	44.2%	57%	–	–
MAML (Finn et al., 2017)	Conv-4-64	48.7±1.8%	63.1±0.9%	58.9±1.9%	71.5±1.0%
Prototypical Net (Snell et al., 2017)	Conv-4-64	49.4±0.8%	68.2±0.7%	55.5±0.7%	72.0±0.6%
Relation Net (Sung et al., 2018)	Conv-4-64	50.4±0.8%	65.3±0.7%	55.0±1.0%	69.3±0.8%
GNN (Satorras & Bruna, 2017)	Conv-4-64	50.3%	66.4%	61.9%	75.3%
R2-D2 (Bertinetto et al., 2018)	Conv-4-64	49.5±0.2%	65.4±0.2%	62.3±0.2%	77.4±0.2%
TPN (Liu et al., 2018)	Conv-4-64	55.5%	69.9%	–	–
Gidaris et al. (2019)	Conv-4-64	54.8±0.4%	**71.9±0.3%**	63.5±0.3%	**79.8±0.2%**
SIB K=0 (*Pre-trained feature*)	Conv-4-64	50.0±0.4%	67.0±0.4%	59.2±0.5%	75.4±0.4%
SIB η=1e-3, K=3	Conv-4-64	**58.0±0.6%**	70.7±0.4%	**68.7±0.6%**	77.1±0.4%
SIB η=1e-3, K=0	Conv-4-128	53.62 ± 0.79%	71.48 ± 0.64%	–	–
SIB η=1e-3, K=1	Conv-4-128	58.74 ± 0.89%	74.12 ± 0.63%	–	–
SIB η=1e-3, K=3	Conv-4-128	62.59 ± 1.02%	75.43 ± 0.67%	–	–
SIB η=1e-3, K=5	Conv-4-128	**63.26 ± 1.07%**	**75.73 ± 0.71%**	–	–
TADAM (Oreshkin et al., 2018)	ResNet-12	58.5±0.3%	76.7±0.3%	–	–
SNAIL (Santoro et al., 2017)	ResNet-12	55.7±1.0%	68.9±0.9%	–	–
MetaOptNet-RR (Lee et al., 2019)	ResNet-12	61.4±0.6%	77.9±0.5%	72.6±0.7%	84.3±0.5%
MetaOptNet-SVM	ResNet-12	62.6±0.6%	78.6±0.5%	72.0±0.7%	84.2±0.5%
CTM (Li et al., 2019)	ResNet-18	64.1±0.8%	**80.5±0.1%**	–	–
Qiao et al. (2018)	WRN-28-10	59.6±0.4%	73.7±0.2%	–	–
LEO (Rusu et al., 2019)	WRN-28-10	61.8±0.1%	77.6±0.1%	–	–
Gidaris et al. (2019)	WRN-28-10	62.9±0.5%	79.9±0.3%	73.6±0.3%	**86.1±0.2%**
SIB K=0 (*Pre-trained feature*)	WRN-28-10	60.6±0.4%	77.5±0.3%	70.0±0.5%	83.5±0.4%
SIB η=1e-3, K=1	WRN-28-10	67.3±0.5%	78.8±0.4%	76.8±0.5%	84.9±0.4%
SIB η=1e-3, K=3	WRN-28-10	69.6±0.6 %	78.9±0.4%	78.4±0.6%	85.3±0.4%
SIB η=1e-3, K=5	WRN-28-10	**70.0±0.6%**	79.2±0.4%	**80.0±0.6%**	85.3±0.4%

Table 1: Average classification accuracies (with 95% confidence intervals) on the test-set of MiniImageNet and CIFAR-FS. For evaluation, we sample 2000 and 5000 episodes respectively for MiniImageNet and CIFAR-FS and test three different architectures as the feature extractor: Conv-4-64, Conv-4-128 and WRN-28-10. We train SIB with learning rate 0.001 and try different numbers of synthetic gradient steps K.

5.1.1 SETUP

Datasets We choose standard benchmarks of few-shot classification for this experiment. Each benchmark is composed of disjoint training, validation and testing classes. **MiniImageNet** is proposed by Vinyals et al. (2016), which contains 100 classes, split into 64 training classes, 16 validation classes and 20 testing classes, where each class consists of 600 image-label pairs and each image is of size 84×84. **CIFAR-FS** is proposed by Bertinetto et al. (2018), which is created by dividing the original CIFAR-100 into 64 training classes, 16 validation classes and 20 testing classes; each image is of size 32×32.

Network architectures Following Gidaris & Komodakis (2018); Qiao et al. (2018); Gidaris et al. (2019), we implement f by a 4-layer convolutional network (Conv-4-64 or Conv-4-128[4]) or a WideResNet (WRN-28-10) (Zagoruyko & Komodakis, 2016). We pretrain the feature network $f(\cdot)$ on the 64 training classes for a stardard 64-way classification. We reuse the feature averaging network proposed by Gidaris & Komodakis (2018) as our initialization network $\lambda(\cdot)$, which basically averages the feature vectors of all data points from the same class and then scales each feature dimension differently by a learned coefficient. For the synthetic gradient network $\xi(\cdot)$, we implement a three-layer MLP with hidden-layer size $8k$. Finally, for the predictor $\hat{y}_{ij}(\cdot, w_i)$, we adopt the cosine-similarity based classifier advocated by Chen et al. (2019) and Gidaris & Komodakis (2018).

Evaluation metrics In few-shot classification, a task (aka episode) t consists of a *query set* d_t and a *support set* d_t^l. When we say the task t is k-*way*-n^l-*shot* we mean that d_t^l is formed by first sampling k classes from a pool of classes; then, for each sampled class, n^l examples are drawn and a new

[4]Conv-4-64 consists of 4 convolutional blocks each implemented with a 3×3 convolutional layer followed by BatchNorm + ReLU + 2×2 max-pooling units. All blocks of Conv-4-64 have 64 feature channels. Conv-4-128 has 64 feature channels in the first two blocks and 128 feature channels in the last two blocks.

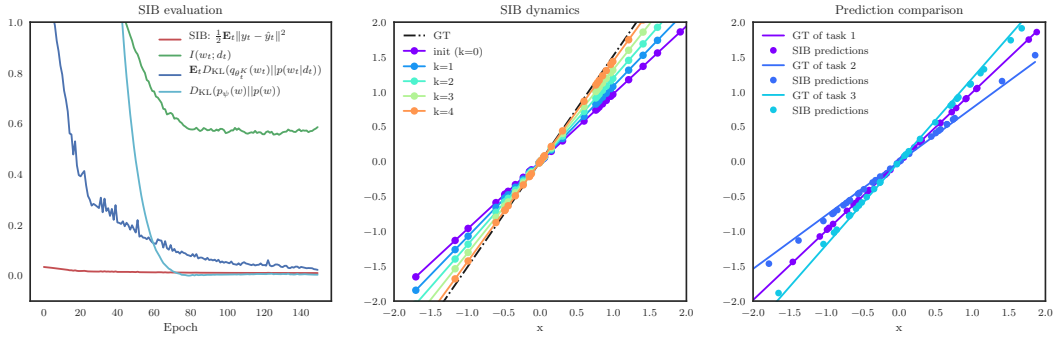

Figure 3: **Left**: the mean-square errors on D_{test}, $\mathbb{E}_t D_{\mathrm{KL}}(q_{\theta_t^K}(w_t)\|p(w_t|d_t))$, $D_{\mathrm{KL}}(p_\psi(w)\|p(w))$ and the estimate of $I(w;d) \approx \mathbb{E}_t D_{\mathrm{KL}}(q_{\theta_t^K}(w_t)\|p_\psi(w_t))$. **Middle**: the predicted y's by $y = \theta_t^k x$ for $k = 0, \ldots, 4$. **Right**: the predictions of SIB.

label taken from $\{0, \ldots, k-1\}$ is assigned to these examples. By default, each query set contains $15k$ examples. The goal of this problem is to predict the labels of the query set, which are provided as ground truth during training. The evaluation is the average classification accuracy on the tasks created with testing classes.

Training details We run SGD with batch size 8 for 40000 steps, where the learning rate is fixed to 10^{-3}. During training, we freeze the feature network. To select the best hyper-parameters, for each dataset, we sample 1000 tasks from the validation classes and reuse them at each training epoch. We use these validation tasks to select the best meta-model and then use it for the final evaluation on the tasks sampled from testing classes.

5.1.2 Comparison to state-of-the-art meta-learning methods

In Table 1, we show a comparison between the state-of-the-art approaches and several variants of our method (varying K or $f(\cdot)$). Apart from SIB, TPN (Liu et al., 2018) and CTM (Li et al., 2019) are also transductive methods.

First of all, comparing SIB ($K = 3$) to SIB ($K = 0$), we observe a clear improvement, which suggests that, by taking a few synthetic gradient steps, we do obtain a better variational posterior as promised. For 1-shot learning, SIB (when $K = 3$ or $K = 5$) significantly outperforms previous methods on both MiniImageNet and CIFAR-FS. For 5-shot learning, the results are also comparable. It should be noted that the performance boost is consistently observed with different feature networks, which suggests that SIB is a general method for few-shot learning.

However, we also observe a potential limitation of SIB: when the support set is relatively large, e.g., 5-shot, with a good feature network like WRN-28-10, the initialization θ_t^0 may already be close to some local minimum, making the updates later less important.

For 5-shot learning, SIB is sligtly worse than CTM (Li et al., 2019) and/or Gidaris et al. (2019). CMT (Li et al., 2019) can be seen as an alternative way to incorporate transduction – it measures the similarity between a query example and the support set while making use of intra- and inter-class relationships. Gidaris et al. (2019) uses in addition the self-supervision as an auxilary loss to learn a richer and more transferable feature model. Both ideas are complementary to SIB. We leave these extensions to our future work.

5.2 Zero-shot regression: spinning lines

Since our variational posterior relies only on x_t, SIB is also applicable to zero-shot problems (i.e., no support set available). We first look at a toy multi-task problem, where $I(w_t; d_t)$ is tractable.

Denote by $D_{\text{train}} := \{d_t\}_{t=1}^N$ the train set, which consists of datasets of size n: $d = \{(x_i, y_i)\}_{i=1}^n$. We construct a dataset d by firstly sampling iid Gaussian random variables as inputs: $x_i \sim \mathcal{N}(\mu, \sigma^2)$. Then, we generate the weight for each dataset by calculating the mean of the inputs and shifting

Method	Art	Cartoon	Sketch	Photo	Average
JiGen (Carlucci et al., 2019)	84.9%	81.1%	79.1%	98.0%	85.7%
Rot (Xu et al., 2019)	88.7%	86.4%	74.9%	98.0%	87.0%
SIB-Rot $K = 0$	85.7%	86.6%	80.3%	98.3%	87.7%
SIB-Rot $K = 3$	**88.9%**	**89.0%**	**82.2%**	**98.3%**	**89.6%**

Table 2: Multi-source domain adaptation results on PACS with ResNet-18 features. Three domains are used as the source domains keeping the fourth one as target.

with a Gaussian random variable ϵ_w: $w = \frac{1}{n}\sum_i x_i + \epsilon_w$, $\epsilon_w \sim \mathcal{N}(\mu_w, \sigma_w^2)$. The output for x_i is $y_i = w \cdot x_i$. We decide ahead of time the hyperparameters $\mu, \sigma, \mu_w, \sigma_w$ for generating x_i and y_i. Recall that a weighted sum of iid Gaussian random variables is still a Gaussian random variable. Specifically, if $w = \sum_i c_i x_i$ and $x_i \sim \mathcal{N}(\mu_i, \sigma_i^2)$, then $w \sim \mathcal{N}(\sum_i c_i \mu_i, \sum_i c_i^2 \sigma_i^2)$. Therefore, we have $p(w) = \mathcal{N}(\mu + \mu_w, \frac{1}{n}\sigma^2 + \sigma_w^2)$. On the other hand, if we are given a dataset d of size n, the only uncertainty about w comes from ϵ_w, that is, we should consider x_i as a constant given d. Therefore, the posterior $p(w|d) = \mathcal{N}(\frac{1}{n}\sum_{i=1}^n x_i + \mu_w, \sigma_w^2)$. We use a simple implementation for SIB:

- the variational posterior is realized by

$$q_{\theta_t^K}(w) = \mathcal{N}(\theta_t^K, \sigma_w),\ \theta_t^{k+1} = \theta_t^k - 10^{-3}\sum_{i=1}^n x_i \xi(\theta_t^k x_i),\ \text{and}\ \theta_t^0 = \lambda \in \mathbb{R}; \tag{16}$$

- ℓ_t is a mean squared error, implies that $p(y|x, w) = \mathcal{N}(wx, 1)$;
- $p_\psi(w)$ is a Gaussian distribution with parameters $\psi \in \mathbb{R}^2$;
- the synthetic gradient network ξ is a three-layer MLP with hidden size 8.

In the experiment, we sample 240 tasks respectively for both D_{train} and D_{test}. We learn SIB and BNN on D_{train} for 150 epochs using the ADAM optimizer (Kingma & Ba, 2014), with learning rate 10^{-3} and batch size 8. Other hyperparameters are specified as follows: $n = 32, K = 3, \mu = 0, \sigma = 1, \mu_w = 1, \sigma_w = 0.1$. The results are shown in Figure 3. On the left, both $D_{\text{KL}}(q_{\theta_t^K}(w_t)\|p(w_t|d_t))$ and $D_{\text{KL}}(p_\psi(w)\|p(w))$ are close to zero indicating the success of the learning. More interestingly, in the middle, we see that $\theta_t^0, \theta_t^1, \ldots, \theta_t^4$ evolves gradually towards the ground truth, which suggests that the synthetic gradient network is able to identify the descent direction after meta-learning.

5.3 Zero-shot classification: unsupervised multi-source domain adaptation

A more interesting zero-shot multi-task problem is unsupervised domain adaptation. We consider the case where there exists multiple source domains and a unlabeled target domain. In this case, we treat each minibatch as a task. This makes sense because the difference in statistics between two minibatches are much larger than in the traditional supervised learning. The experimental setup is similar to few-shot classification described in Section 5.1, except that we do not have a support set and the class labels between two tasks are the same. Hence, it is possible to explore the relationship between class labels and *self-supervised* labels to implement the initialization network λ without resorting to support set. We reuse the same model implementation for SIB as described in Section 5.1. The only difference is the initialization network. Denote by $z_t := \{z_{t,i}\}_{i=1}^n$ the set of self-supervised labels of task t, the initialization network λ is implemented as follows:

$$\theta_t^0 = \lambda - \eta\, \nabla_\theta L_t\Big(\hat{z}_t\big(\hat{y}_t(f(x_t), w_t(\theta, \epsilon)), f(x_t)\big), z_t\Big), \tag{17}$$

where λ[5] is a global initialization similar to the one used by MAML; L_t is the self-supervised loss, $\hat{z}_t$ is the set of predictions of the self-supervised labels. One may argue that $\theta_t^0 = \lambda$ would be a simpler solution. However, it is insufficient since the gap between two domains can be very large. The initial solution yielded by (17) is more dynamic in the sense that θ_t^0 is adapted taking into account the information from x_t.

[5] λ is overloaded to be both the network and its parameters.

In terms of experiments, we test SIB on the PACS dataset (Li et al., 2017a), which has 7 object categories and 4 domains (Photo, Art Paintings, Cartoon and Sketches), and compare with state-of-the-art algorithms for unsupervised domain adaptation. We follow the standard experimental setting (Carlucci et al., 2019), where the feature network is implemented by ResNet-18. We assign a self-supervised label $z_{t,i}$ to image i by rotating the image by a predicted degree. This idea was originally proposed by Gidaris et al. (2018) for representation learning and adopted by Xu et al. (2019) for domain adaptation. The training is done by running ADAM for 60 epochs with learning rate 10^{-4}. We take each domain in turns as the target domain. The results are shown in Table 2. It can be seen that SIB-Rot ($K = 3$) improves upon the baseline SIB-Rot ($K = 0$) for zero-shot classification, which also outperforms state-of-the-art methods when the baseline is comparable.

6 Conclusion

We have presented an empirical Bayesian framework for meta-learning. To enable an efficient variational inference, we followed the amortized inference paradigm, and proposed to use a transductive scheme for constructing the variational posterior. To implement the transductive inference, we make use of two neural networks: a synthetic gradient network and an initialization network, which together enables a synthetic gradient descent on the unlabeled data to generate the parameters of the amortized variational posterior dynamically. We have studied the theoretical properties of the proposed framework and shown that it yields performance boost on MiniImageNet and CIFAR-FS for few-shot classification.

References

Alessandro Achille and Stefano Soatto. Emergence of invariance and disentangling in deep representations. *arXiv preprint arXiv:1706.01350*, 2017.

Ron Amit and Ron Meir. Meta-learning by adjusting priors based on extended pac-bayes theory. In *International Conference on Machine Learning*, pp. 205–214, 2018.

Y Bengio, S Bengio, and J Cloutier. Learning a synaptic learning rule. In *IJCNN-91-Seattle International Joint Conference on Neural Networks*, volume 2, pp. 969–vol. IEEE, 1991.

James O. Berger. *Statistical Decision Theory and Bayesian Analysis*. Springer-Verlag New York, 1985.

Luca Bertinetto, João F. Henriques, Philip H. S. Torr, and Andrea Vedaldi. Meta-learning with differentiable closed-form solvers. *ArXiv*, abs/1805.08136, 2018.

Fabio M Carlucci, Antonio D'Innocente, Silvia Bucci, Barbara Caputo, and Tatiana Tommasi. Domain generalization by solving jigsaw puzzles. In *Proceedings of the IEEE Conference on Computer Vision and Pattern Recognition*, pp. 2229–2238, 2019.

O Chapelle, B Schölkopf, and A Zien. A discussion of semi-supervised learning and transduction. *Semi-Supervised Learning*, pp. 457–462, 2006.

Wei-Yu Chen, Yen-Cheng Liu, Zsolt Kira, Yu-Chiang Frank Wang, and Jia-Bin Huang. A closer look at few-shot classification. *arXiv preprint arXiv:1904.04232*, 2019.

Jacob Devlin, Ming-Wei Chang, Kenton Lee, and Kristina Toutanova. Bert: Pre-training of deep bidirectional transformers for language understanding. *arXiv preprint arXiv:1810.04805*, 2018.

Chelsea Finn, Pieter Abbeel, and Sergey Levine. Model-agnostic meta-learning for fast adaptation of deep networks. In *Proceedings of the 34th International Conference on Machine Learning-Volume 70*, pp. 1126–1135. JMLR. org, 2017.

Sebastian Flennerhag, Pablo G Moreno, Neil D Lawrence, and Andreas Damianou. Transferring knowledge across learning processes. *International Conference on Learning Representations (ICLR)*, 2019.

Marta Garnelo, Jonathan Schwarz, Dan Rosenbaum, Fabio Viola, Danilo J Rezende, SM Eslami, and Yee Whye Teh. Neural processes. *arXiv preprint arXiv:1807.01622*, 2018.

Spyros Gidaris and Nikos Komodakis. Dynamic few-shot visual learning without forgetting. In *Proceedings of the IEEE Conference on Computer Vision and Pattern Recognition*, pp. 4367–4375, 2018.

Spyros Gidaris, Praveer Singh, and Nikos Komodakis. Unsupervised representation learning by predicting image rotations. *arXiv preprint arXiv:1803.07728*, 2018.

Spyros Gidaris, Andrei Bursuc, Nikos Komodakis, Patrick Pérez, and Matthieu Cord. Boosting few-shot visual learning with self-supervision. *arXiv preprint arXiv:1906.05186*, 2019.

Irving John Good. Some history of the hierarchical bayesian methodology. *Trabajos de estadística y de investigación operativa*, 31(1):489, 1980.

Erin Grant, Chelsea Finn, Sergey Levine, Trevor Darrell, and Thomas Griffiths. Recasting gradient-based meta-learning as hierarchical bayes. *arXiv preprint arXiv:1801.08930*, 2018.

Kaiming He, Xiangyu Zhang, Shaoqing Ren, and Jian Sun. Delving deep into rectifiers: Surpassing human-level performance on imagenet classification. In *Proceedings of the IEEE international conference on computer vision*, pp. 1026–1034, 2015.

Sergey Ioffe and Christian Szegedy. Batch normalization: Accelerating deep network training by reducing internal covariate shift. *arXiv preprint arXiv:1502.03167*, 2015.

Max Jaderberg, Wojciech Marian Czarnecki, Simon Osindero, Oriol Vinyals, Alex Graves, David Silver, and Koray Kavukcuoglu. Decoupled neural interfaces using synthetic gradients. In *Proceedings of the 34th International Conference on Machine Learning-Volume 70*, pp. 1627–1635. JMLR, 2017.

Hyunjik Kim, Andriy Mnih, Jonathan Schwarz, Marta Garnelo, Ali Eslami, Dan Rosenbaum, Oriol Vinyals, and Yee Whye Teh. Attentive neural processes. *arXiv preprint arXiv:1901.05761*, 2019.

Diederik P Kingma and Jimmy Ba. Adam: A method for stochastic optimization. *arXiv preprint arXiv:1412.6980*, 2014.

Diederik P Kingma and Max Welling. Auto-encoding variational bayes. *arXiv preprint arXiv:1312.6114*, 2013.

Alp Kucukelbir and David M Blei. Population empirical bayes. *arXiv preprint arXiv:1411.0292*, 2014.

Kwonjoon Lee, Subhransu Maji, Avinash Ravichandran, and Stefano Soatto. Meta-learning with differentiable convex optimization. In *CVPR*, 2019.

Da Li, Yongxin Yang, Yi-Zhe Song, and Timothy M Hospedales. Deeper, broader and artier domain generalization. In *Proceedings of the IEEE International Conference on Computer Vision*, pp. 5542–5550, 2017a.

Hongyang Li, David Eigen, Samuel Dodge, Matthew Zeiler, and Xiaogang Wang. Finding Task-Relevant Features for Few-Shot Learning by Category Traversal. In *CVPR*, 2019.

Zhenguo Li, Fengwei Zhou, Fei Chen, and Hang Li. Meta-sgd: Learning to learn quickly for few-shot learning. *arXiv preprint arXiv:1707.09835*, 2017b.

Yanbin Liu, Juho Lee, Minseop Park, Saehoon Kim, Eunho Yang, Sung Ju Hwang, and Yi Yang. Learning to propagate labels: Transductive propagation network for few-shot learning. *arXiv preprint arXiv:1805.10002*, 2018.

Alireza Makhzani, Jonathon Shlens, Navdeep Jaitly, Ian Goodfellow, and Brendan Frey. Adversarial autoencoders. *arXiv preprint arXiv:1511.05644*, 2015.

Tom Minka. Discriminative models, not discriminative training. Technical report, Technical Report MSR-TR-2005-144, Microsoft Research, 2005.

Alex Nichol, Joshua Achiam, and John Schulman. On first-order meta-learning algorithms. *arXiv preprint arXiv:1803.02999*, 2018.

Boris N. Oreshkin, Pau Rodríguez López, and Alexandre Lacoste. Tadam: Task dependent adaptive metric for improved few-shot learning. In *Advances in Neural Information Processing Systems (NIPS)*, 2018.

Siyuan Qiao, Chenxi Liu, Wei Shen, and Alan L Yuille. Few-shot image recognition by predicting parameters from activations. In *Proceedings of the IEEE Conference on Computer Vision and Pattern Recognition*, pp. 7229–7238, 2018.

Sachin Ravi and Alex Beatson. Amortized bayesian meta-learning. *International Conference on Learning Representation*, 2018.

Sachin Ravi and Hugo Larochelle. Optimization as a model for few-shot learning. *International Conference on Learning Representation*, 2016.

Danilo Jimenez Rezende, Shakir Mohamed, and Daan Wierstra. Stochastic backpropagation and approximate inference in deep generative models. *arXiv preprint arXiv:1401.4082*, 2014.

Herbert Robbins. An empirical bayes approach to statistics. In *Herbert Robbins Selected Papers*, pp. 41–47. Springer, 1985.

Andrei A. Rusu, Dushyant Rao, Jakub Sygnowski, Oriol Vinyals, Razvan Pascanu, Simon Osindero, and Raia Hadsell. Meta-learning with latent embedding optimization. In *International Conference on Learning Representations*, 2019. URL `https://openreview.net/forum?id=BJgklhAcK7`.

Adam Santoro, David Raposo, David G. T. Barrett, Mateusz Malinowski, Razvan Pascanu, Peter W. Battaglia, and Timothy P. Lillicrap. A simple neural network module for relational reasoning. In *NIPS*, 2017.

Victor Garcia Satorras and Joan Bruna. Few-shot learning with graph neural networks. *ArXiv*, abs/1711.04043, 2017.

Jurgen Schmidhuber. Evolutionary principles in self-referential learning. on learning now to learn: The meta-meta-meta...-hook. Phd thesis, Technische Universitat Munchen, Germany, 1987. URL `http://www.idsia.ch/~juergen/diploma.html`.

Jake Snell, Kevin Swersky, and Richard Zemel. Prototypical networks for few-shot learning. In *Advances in Neural Information Processing Systems*, pp. 4077–4087, 2017.

Flood Sung, Yongxin Yang, Li Zhang, Tao Xiang, Philip HS Torr, and Timothy M Hospedales. Learning to compare: Relation network for few-shot learning. In *Proceedings of the IEEE Conference on Computer Vision and Pattern Recognition*, 2018.

Sebastian Thrun and Lorien Pratt. *Learning to learn*. Kluwer Academic Publishers, 1998.

Naftali Tishby, Fernando C Pereira, and William Bialek. The information bottleneck method. *arXiv preprint physics/0004057*, 2000.

Jakub M Tomczak and Max Welling. Vae with a vampprior. *arXiv preprint arXiv:1705.07120*, 2017.

Oriol Vinyals, Charles Blundell, Timothy Lillicrap, koray kavukcuoglu, and Daan Wierstra. Matching networks for one shot learning. In *Advances in Neural Information Processing Systems 29*, pp. 3630–3638. Curran Associates, Inc., 2016.

Aolin Xu and Maxim Raginsky. Information-theoretic analysis of generalization capability of learning algorithms. In *Advances in Neural Information Processing Systems*, pp. 2524–2533, 2017.

Jiaolong Xu, Liang Xiao, and Antonio M López. Self-supervised domain adaptation for computer vision tasks. *IEEE Access*, 7:156694–156706, 2019.

Sergey Zagoruyko and Nikos Komodakis. Wide residual networks. *arXiv preprint arXiv:1605.07146*, 2016.

Xiaojin Zhu, Zoubin Ghahramani, and John D Lafferty. Semi-supervised learning using gaussian fields and harmonic functions. In *Proceedings of the 20th International conference on Machine learning (ICML-03)*, pp. 912–919, 2003.

APPENDIX

A DECOMPOSITION IMPLIED BY EMPIRICAL BAYES

In this section, we prove the statement in (10). First of all,

$$\begin{aligned} p_{\psi,f}(w_1,\ldots,w_N,\mathcal{D}) &= p_{\psi,f}(w_1,\ldots,w_N \mid \mathcal{D}) p_{\psi,f}(\mathcal{D}) \\ &= p_{\psi,f}(w_1,\ldots,w_N \mid \mathcal{D}) \prod_{t=1}^{N} p_{\psi,f}(d_t) \end{aligned} \tag{18}$$

Then, we only need to show

$$\begin{aligned} p_{\psi,f}(w_1,\ldots,w_N|\mathcal{D}) &= \frac{\prod_{t=1}^{N} p_f(d_t|w_t)p_\psi(w_t)}{\int_{w_1,\ldots,w_N} \prod_{t=1}^{N} p_f(d_t|w_t)p_\psi(w_t)} \\ &= \frac{\prod_{t=1}^{N} p_f(d_t|w_t)p_\psi(w_t)}{\prod_{t=1}^{N} \int_{w_t} p_f(d_t|w_t)p_\psi(w_t)} = \prod_{t=1}^{N} p_{\psi,f}(w_t|d_t). \end{aligned} \tag{19}$$

B PROOF OF THEOREM 1

Before going into details, we first introduce a few notations, definitions, and a technical lemma.

- The *entropy* is defined as $H_p(\mathrm{x}) := \mathbb{E}_{p(\mathrm{x})}[-\log p(\mathrm{x})]$;
- The *mutual information* is given by $I_p(\mathrm{x};\mathrm{y}) := D_{\mathrm{KL}}\big(p(\mathrm{x},\mathrm{y})\|p(\mathrm{x})p(\mathrm{y})\big)$.
- Very often, we decompose the mutual information as $I_p(\mathrm{x};\mathrm{y}) = H_p(\mathrm{x}) - H_p(\mathrm{x}|\mathrm{y})$ with $H_p(\mathrm{x}|\mathrm{y}) := \mathbb{E}_{p(\mathrm{x},\mathrm{y})}[-\log p(\mathrm{x}|\mathrm{y})]$ the *conditional entropy*.
- The *cross entropy* is defined as $H_{p,q}(\mathrm{x}) := \mathbb{E}_{p(\mathrm{x})}[-\log q(\mathrm{x})]$. Similarly, we have the *cross conditional entropy* $H_{p,q}(\mathrm{x}|\mathrm{y}) := \mathbb{E}_{p(\mathrm{x},\mathrm{y})}[-\log q(\mathrm{x}|\mathrm{y})]$ and the *cross mutual information* $I_{p,q}(\mathrm{x};\mathrm{y}) = H_{p,q}(\mathrm{x}) - H_{p,q}(\mathrm{x}|\mathrm{y})$.

Definition 1. *A random variable* x *is subgaussian if there exists a positive number* σ *such that* $\mathbb{E}[\exp(\lambda(\mathrm{x}-\mathbb{E}\mathrm{x}))] \le \exp(\sigma^2\lambda^2/2)$ *for all* $\lambda \in \mathbb{R}$.

Lemma 1 (Xu & Raginsky (2017))**.** *If g(*x, y*) is* σ*-subgaussian, then*

$$\big|\mathbb{E}_{p(\mathrm{x},\mathrm{y})} g(\mathrm{x},\mathrm{y}) - \mathbb{E}_{p(\mathrm{x})p(\mathrm{y})} g(\mathrm{x},\mathrm{y})\big| \le \sqrt{2\sigma^2 I_p(\mathrm{x};\mathrm{y})}.$$

Now, we are ready to prove Theorem 1.

Proof. The expected KL divergence can be rewritten as follows:

$$\begin{aligned} &\mathbb{E}_{q(d)} D_{\mathrm{KL}}\Big(q(w|d)\|p(w|d)\Big) = \mathbb{E}_{q(d)}\mathbb{E}_{q(w|d)}\Big[\log \frac{q(w|d)p(d)q(w)}{p(d|w)p(w)q(w)}\Big] \\ &= \mathbb{E}_{q(d)}\mathbb{E}_{q(w|d)}\Big[\log \frac{q(w|d)}{q(w)}\Big] + \mathbb{E}_{q(d)}\mathbb{E}_{q(w|d)}\Big[-\log p(d|w)\Big] \\ &\quad + \mathbb{E}_{q(w)}\Big[\log \frac{q(w)}{p(w)}\Big] + \mathbb{E}_{q(d)}\mathbb{E}_{q(w|d)}\Big[\log p(d)\Big] \\ &= I_q(w;d) + H_{q,p}(d|w) + D_{\mathrm{KL}}\big(q(w)\big\|p(w)\big) - H_{q,p}(d) \qquad (20) \\ &= I_q(w;d) - I_{q,p}(d;w) + D_{\mathrm{KL}}\big(q(w)\big\|p(w)\big) \\ &\ge I_q(w;d) - I_{q,p}(d;w) = I_q(w;d) - I_{q,p}(w;d). \qquad (21) \end{aligned}$$

Note that $I_{q,p}(d;w) = I_{q,p}(w;d)$ and $D_{\mathrm{KL}}\big(q(w)\big\|p(w)\big) = 0$ iff $q(w) = \mathbb{E}_{q(d)}q(w|d) = p(w)$. Similarly, we have

$$\mathbb{E}_{q(d)} D_{\mathrm{KL}}\Big(q(w|d)\|p(d|w)p(w)\Big) \ge I_q(w;d) + H_{q,p}(d|w). \tag{22}$$

by removing the term $H_{q,p}(d)$.

Let us rewrite (20) as

$$\begin{aligned}(20) &= I_q(w;d) + \mathbb{E}_{q(w)} D_{\mathrm{KL}}\big(q(d|w)\|p(d|w)\big) + H_q(d|w) + D_{\mathrm{KL}}\big(q(w)\big\|p(w)\big) - H_{q,p}(d) \\ &= H_q(d) + D_{\mathrm{KL}}\mathbb{E}_{q(w)}\big(q(d|w)\|p(d|w)\big) + D_{\mathrm{KL}}\big(q(w)\big\|p(w)\big) - H_{q,p}(d) \\ &= -D_{\mathrm{KL}}\big(q(d)\|p(d)\big) + \mathbb{E}_{q(w)} D_{\mathrm{KL}}\big(q(d|w)\|p(d|w)\big) + D_{\mathrm{KL}}\big(q(w)\big\|p(w)\big) \\ &\leq \mathbb{E}_{q(w)} D_{\mathrm{KL}}\big(q(d|w)\|p(d|w)\big) + D_{\mathrm{KL}}\big(q(w)\big\|p(w)\big) = D_{\mathrm{KL}}\Big(q(w,d)\|p(w,d)\Big), \end{aligned} \tag{23}$$

which attains the right hand side of the second inequality.

Recall that $L(w,d) := \frac{1}{n}\sum_{i=1}^n \ell_t(\hat{y}_i(f(x_i),w),y_i)$. If $\ell_t(\hat{y}_i(f(x_i),w),y_i)$ is σ-subgaussian for all w, then $L(w,d)$ is $\sigma/\sqrt{n}$-subgaussian due to the iid assumption on d. Thus, by Lemma 1, we have

$$\big|\mathrm{gen}(q(w|d),q(d))\big| \leq \sqrt{\frac{2\sigma^2}{n} I_q(w;d)}.$$

On the other hand, $H_{q,p}(d|w) = \hat{R}(q(w|d),q(d))$. Combining both, we have

$$\frac{n}{2\sigma^2}\mathrm{gen}(q(w|d),q(d))^2 + \hat{R}(q(w|d),q(d)) \leq I_q(w;d) + H_{q,p}(d|w)$$

as desired. □

Recall that information bottleneck (IB) involves an optimization

$$\min_{q(w|d)} I_q(w;d) - \beta\, I_{q,p}(w;d) \text{ with } \beta > 0. \tag{24}$$

Thus, we have established a connection between local empirical Bayes and information bottleneck. The idea of IB is to view w as a compressed representation of d from a *rate-distortion perspective*:

- $I_q(w;d)$ is known as *rate*, which is a regularization term discouraging memorization;
- $-I_{q,p}(w;d) = H_{q,p}(d|w) - H_{q,p}(d)$ is naturally a measure of *distortion* since $H_{q,p}(d|w)$ is equal to the expected negative log-likelihood and $H_{q,p}(d)$ is a constant wrt $q(w|d)$.

Thus, solving (7) amounts to minimizing an upper bound of the IB objective if we generalize the posterior as follows:

$$p_\psi(w|d) = \frac{p(d|w)^\beta p_\psi(w)}{\int_w p(d|w)^\beta p_\psi(w)} \text{ with } \beta > 0. \tag{25}$$

C Importance of synthetic gradients

To further verify the effectiveness of the synthetic gradient descent, we implement an inductive version of SIB inspired by MAML, where the initialization θ_t^0 is generated exactly the same way as SIB using $\lambda(d_t^l)$, but it then follows the iterations in (6) as in MAML rather than follows the iterations in (9) as in standard SIB.

We conduct an experiment on CIFAR-FS using Conv-4-64 feature network. The results are shown in Table 3. It can be seen that there is no improvement over SIB ($K = 0$) suggesting that the inductive approach is insufficient.

D Varying n

We notice that changing the size of d_t (i.e., n) during training does make a difference on testing.

		inductive SIB		**SIB**			
		Training on 1-shot		**Training on 1-shot**		**Training on 5-shot**	
		Testing on		**Testing on**		**Testing on**	
K	η	1-shot	5-shot	1-shot	5-shot	1-shot	5-shot
0	-	59.7±0.5%	75.5±0.4%	59.2±0.5%	75.4±0.4%	59.2±0.5%	75.4±0.4%
1	1e-1	59.8±0.5%	71.2±0.4%	65.3±0.6%	75.8±0.4%	64.5±0.6%	77.3±0.4%
3	1e-1	59.6±0.5%	75.9±0.4%	65.0±0.6%	75.0±0.4%	64.0±0.6%	77.0±0.4%
5	1e-1	59.9±0.5%	74.9±0.4%	66.0±0.6%	76.3±0.4%	64.0±0.5%	76.8±0.4%
1	1e-2	59.7±0.5%	75.5±0.4%	67.8±0.6%	74.3±0.4%	63.6±0.6%	77.3±0.4%
3	1e-2	59.5±0.5%	75.8±0.4%	68.6±0.6%	77.4±0.4%	67.8±0.6%	78.5±0.4%
5	1e-2	59.8±0.5%	75.7±0.4%	67.4±0.6%	72.6±0.6%	67.7±0.7%	77.7±0.4%
1	1e-3	59.5±0.5%	75.6±0.4%	66.2±0.6%	75.7±0.4%	64.6±0.6%	78.1±0.4%
3	1e-3	59.9±0.5%	75.9±0.4%	68.7±0.6%	77.1±0.4%	66.8±0.6%	78.4±0.4%
5	1e-3	59.4±0.5%	75.7±0.4%	69.1±0.6%	76.7±0.4%	66.7±0.6%	78.5±0.4%
1	1e-4	58.8±0.5%	75.5±0.4%	59.0±0.5%	75.7±0.4%	59.3±0.5%	75.7±0.4%
3	1e-4	59.4±0.5%	75.9±0.4%	58.9±0.5%	75.6±0.4%	59.3±0.5%	75.9±0.4%
5	1e-4	59.3±0.5%	75.3±0.4%	60.1±0.5%	76.0±0.4%	60.5±0.5%	76.4±0.4%

Table 3: Average 5-way classification accuracies (with 95% confidence intervals) with Conv-4-64 on the test set of CIFAR-FS. For each test, we sample 5000 episodes containing 5 categories (5-way) and 15 queries in each category. We report the results with using different learning rate η as well as different number of updates K. Note that $K = 0$ is the performance only using the pre-trained feature.

n	5-way, 5-shot		5-way, 1-shot	
	Validation	Test	Validation	Test
3	77.97 ± 0.34%	75.91 ± 0.66%	63.60 ± 0.52%	61.32 ± 1.02%
5	78.14 ± 0.35%	76.01 ± 0.66%	64.67 ± 0.55%	62.50 ± 1.02%
10	**78.30 ± 0.35%**	**76.22 ± 0.66%**	**65.34 ± 0.56%**	**63.22 ± 1.04%**
15	77.53 ± 0.35%	75.43 ± 0.67%	65.14 ± 0.55%	62.59 ± 1.02%
30	76.21 ± 0.35%	74.04 ± 0.67%	63.37 ± 0.53%	60.96 ± 0.98%
45	75.65 ± 0.36%	73.27 ± 0.66%	62.08 ± 0.51%	59.59 ± 0.93%

Table 4: Average classification accuracies on the validation set and the test set of Mini-ImageNet with backbone Conv-4-128. We modify the number of query images, i.e., n, for each episode to study the effect on generalization.